UNIVERSITY OF CALIFORNIA
Santa Barbara

Visual Terrain Classification For Legged Robots

A Thesis submitted in partial satisfaction
of the requirements for the degree of

Master of Science

in

Electrical and Computer Engineering

by

Paul Filitchkin

December 2011

The Thesis of
Paul Filitchkin is approved:

Professor Joao Hespanha

Professor B.S. Manjunath

Professor Katie Byl, Committee Chairperson

September 2011

Abstract

Visual Terrain Classification For Legged Robots

Paul Filitchkin

Recent work in terrain classification has relied largely on 3D sensing methods and color based classification. We present an approach that works with a single, compact camera and maintains high classification rates that are robust to changes in illumination. Terrain is classified using a bag of visual words (BOVW) created from speeded up robust features (SURF) with a support vector machine (SVM) classifier. We present several novel techniques to augment this approach. A gradient descent inspired algorithm is used to adjust the SURF Hessian threshold to reach a nominal feature density. A sliding window technique is also used to classify mixed terrain images with high resolution. We demonstrate that our approach is suitable for small legged robots by performing real-time terrain classification on LittleDog. The classifier is used to select between predetermined gaits for traversing terrain of varying difficulty. Results indicate that real-time classification in the loop is faster than using a single all-terrain gait.

Contents

List of Figures

List of Tables

Chapter 1

Terrain Classification

1.1 Introduction

Terrain classification is a vital component of autonomous outdoor navigation, and serves as the test bed for state-of-the-art computer vision and machine learning algorithms. This area of research has gained much popularity from the DARPA Grand Challenge [23] as well as the Mars Exploration Rovers [6].

Recent terrain classification and navigation research has focused on using a combination of 3D sensors and visual data [23] as well as stereo cameras [7] [16]. The work in [5] uses vibration data from onboard sensors for classifying terrain. Most of this work has been applied to wheeled robots, and other test platforms have included a tracked vehicle [15] and a hexapod robot [7]. On the computer vision spectrum of research, interest in terrain classification has been around as early as 1976 [24] for categorizing satellite imagery. More recent work has focused on the generalized problem of recognizing texture. Terrain and texture classification falls into the following categories: spectral-based [13] [22] [21] [1], color-based [23] [8], and feature-based [2].

Over the last decade, a large volume of work has been published on scale invariant feature recognition and classification. Scale invariant features have proven to be very repeatable in images of objects with varying lighting, viewing angle, and size. They are robust to noise and provide very distinctive descriptors for identification. They are suitable for both specific object recognition [18] [11] [19] as well as broad categorization [9] [10].

1.1.1 Executive Summary

In this work we use the SURF algorithm to extract features from terrain, a bag of visual words to describe the features, and a support vector machine to classify the visual words. Using this approach we were able to identify, with up to 95% verification accuracy, 6 different terrain types as shown in Figure 1.1(a). Our method was also able to maintain high verification accuracy with changes in illumination whereas color-based classification performed much worse. We also tested a novel approach for regionally classifying heterogeneous (mixed) terrain images. A support vector machine classifier trained on homogeneous terrain images was used to classify regions on the images. A voting procedure was then used to determine the class of each pixel.

Real-time classification of homogeneous terrain was performed using the LittleDog quadruped robot. Terrain classification was used to select one of three predetermined gaits for traversing 5 different types of terrain. We were able to show that classification in-the-loop with dynamic gait selection allowed the robot to traverse terrain faster than using an all-purpose gait (Gait C) 1.1(b). Traversing the most difficult terrain actually required the all-purpose gait so in that particular case the classification slowed the robot.

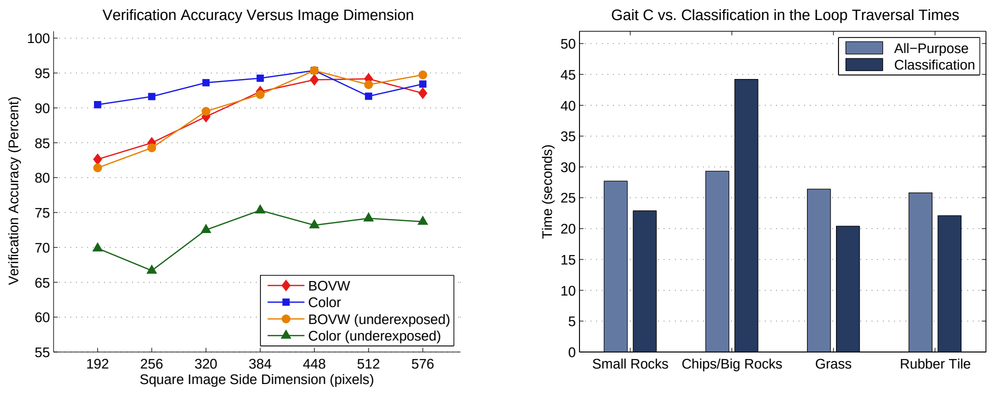

Figure 1.1: Executive Summary of Results

1.2 Terminology

This work uses terminology from machine learning and computer vision along with a few non-standard terms that have been adapted for this application. This section includes an overview of key terms and their meanings. Many image classification techniques were historically adapted from natural language processing and text categorization. For the interested reader, Chapter 16 in [17] provides an introduction to this field.

A **supervised learning** framework is applied in this paper where a set of labeled data is used to train a classifier in an offline environment. Verification is then performed on the classifier by using a different set of labeled test data. Image classification is accomplished by first preprocessing an image, $I \in \mathbb{R}^{m \times n}$, to generate a vector $\mathbf{x} \in \mathbb{R}^M$ which compactly describes the image. The vector becomes the input to the classifier $f(\cdot)$ which outputs a label $\ell_i \in L$, in the form $f(\mathbf{x}) = \ell_i$. Where $L \subset \mathbb{Z}$ and ℓ_i is mapped to some description of the class where i is the index of the class. The most basic example of this approach is to compute the color histogram of an image and use a naïve Bayesian network to determine the class.

In this text, we focus on using features to describe an image. A **feature** is a unique point of interest on an image with an accompanying set of information.

For the purpose of this work, it is implied that each feature consists of a key point and a descriptor. The **key point** includes information such as the pixel coordinate, scale, and orientation. The descriptor (also referred to as a feature vector), $\mathbf{d} \in \mathbb{R}^N$, contains real values that uniquely describe a neighborhood local to a key point. Two popular methods for generating features include **scale invariant feature transform (SIFT)** [14] and **speed up robust features (SURF)** [4]. Each algorithm maintains some degree of invariance to scale, in-plane rotation, noise, and illumination. Both algorithms were used in initial testing for this work, and the SURF algorithm was found to have better speed and slightly better verification accuracy. This is a well established result that was initially reported by Bay et. al. in [4]. Throughout the remainder of this work we will focus primarily on SURF, and unless specified otherwise, the term feature will be used to imply a key point and 64-element descriptor pair generated by the SURF algorithm. The process of **feature extraction** is broken up into two steps: feature detection and feature computation. **Feature detection** consists of finding stable key points in the image and **feature computation** is the process of creating descriptors for each key point.

In this context a **visual word** is a descriptor, $\mathbf{v} \in \mathbb{R}^M$ from a finite set V, that can be used to approximate an image descriptor, $\mathbf{x} \in \mathbb{R}^M$. Each image descriptor can be mapped to the ith visual word $\mathbf{v}_i$ such that $\mathbf{v}_i \longleftrightarrow \mathbf{x}$. The set V is called the **vocabulary** (or visual vocabulary). In this work we use the **bag of visual words (BOVW)** data structure to describe each image (also commonly referred to as a bag of features or a bag of key points). This data structure discards ordering and spatial information and as a result no geometric correspondence between key points and descriptors is preserved. We represent the BOVW by a histogram that tallies the number of times a word appears in a particular image.

In this work the classification problem is separated into two categories: classifying homogeneous and heterogeneous images. A **homogeneous** image is one that contains a single type of terrain and is assigned one class label whereas in a **heterogeneous** context the image contains different patches of terrain that each have a corresponding label. The term **populate** takes on a non-standard definition throughout this work and is used to mean the process of generating or loading data. In particular, the term is used to describe the process of loading cached data from disk if it exists or otherwise computing it from scratch.

1.3 Algorithms

1.3.1 Feature Extraction

In this work we use SURF features for classification. The process of extracting features starts by detecting key points at unique locations on the image. Areas of high contrast such as T-junctions, corners, and blobs are selected and then the neighborhood around each point are used to compute the descriptor. SURF relies on a fast-Hessian detector and selects a region around each key point to compute the descriptor. The descriptor is created using the Haar wavelet response in the horizontal and vertical direction. More details on this process are available in [4].

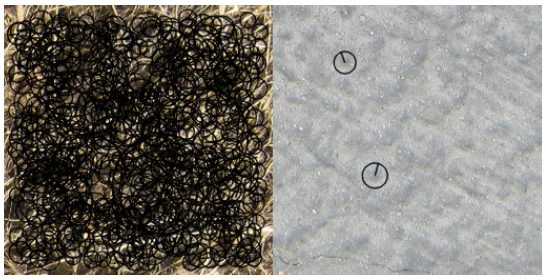

Figure 1.2: High Feature Count Variance Using a Constant Hessian Threshold

A pitfall of using a constant Hessian threshold for detection, especially for images of varying frequency content, is the large variance in the number of key points. Figure 1.2 shows SURF key points for two images with the same parameters. A threshold that is too high may lead to a BOVW with very little data and threshold that is too low will flood the classifier with redundant information and noise. In order to combat this problem we propose a gradient descent inspired threshold adjuster. Let $n = d(h)$ where $d(\cdot)$ is an unknown function that returns the number of key points, n, for a given Hessian threshold h. While the rate of change is not known, $d(\cdot)$ is a monotonically decreasing function. To find the threshold that produces a desired key point count, h', an iterative convex optimization is performed. For a given step i the error can be written as $e(i) = d(h_i) - d(h')$ and our goal is to minimize this quantity. We use an update method similar to gradient descent, but instead of computing the function's gradient we use the error value divided by the local rate of changes, $\frac{e(i)}{|h_i - h_{i-1}|}$. Equation 1.1 is the threshold update step where α is a user set value that determines the update rate.

$$h_{i+1} = h_i + \alpha \frac{d(h_i) - d(h')}{|h_i - h_{i-1}|} \tag{1.1}$$

In practice this approach has the potential to overshoot the target key point count, $d(h')$, by changing the threshold too rapidly. When an overshoot condition is detected, the new threshold becomes the average of the previous two and the update rate is halved.

1.3.2 Generating a Vocabulary

To generate a vocabulary, we use the k-means clustering algorithm with the initialization procedure outlined in [3]. In the context of this work, the k-means problem is to find an integer number of centers that best describe groupings of descriptor data. More formally: let $k \in \mathbb{Z}$ be the desired number of clusters and let $X \subset \mathbb{R}^M$ be the set of descriptors. The goal is to find k centers (descriptors) in $C \subset \mathbb{R}^M$ that minimize ϕ (Equation 1.2).

$$\phi = \sum_{\mathbf{x} \in X} \min_{\mathbf{c} \in C} ||\mathbf{x} - \mathbf{c}||^2 \tag{1.2}$$

The iterative k-means algorithm (Lloyd's algorithm) for achieving this operates as follows: given centers C assign each descriptor $\mathbf{x} \in X$ to the $\mathbf{c} \in C$ that has the smallest Euclidean distance. Then each center is repeatedly recomputed until the centers stop shifting. This procedure will always terminate, but in practice it is common to set a maximum allowable number of iterations. The work in [3] provides an effective initialization procedure that decreases computation time. The authors call this algorithm k-means++ which uses a probabilistic initialization procedure followed by Lloyd's algorithm. In k-means++ the initial center $\mathbf{c}_1 \in C$ is chosen uniformly at random from X and subsequent points $\mathbf{c}_i$ are chosen with the probability in Equation 1.3. Where $D(\mathbf{x})$ is the distance between $\mathbf{x}$ and the nearest center $\mathbf{c}_j$ that has already been chosen $(0 < j < i)$.

$$P(\mathbf{c}_i = \mathbf{x}' \in X) = \frac{D(\mathbf{x}')^2}{\sum_{\mathbf{x} \in X} D(\mathbf{x})^2} \tag{1.3}$$

This approach tends to select centers that are further away from the ones that have already been chosen. The idea is to keep a high variance within the centers, but maintain some probability of not always choosing the furthest point.

1.3.3 Homogeneous Classification

Once a visual vocabulary has been created each image can be described by a word frequency vector. First, a vocabulary word $\mathbf{v}_i$ is assigned to each descriptor $\mathbf{d}_j$ in the image by choosing the i that minimizes $||\mathbf{v}_i - \mathbf{d}_j||$. This process essentially approximates each descriptor with the vocabulary word that has the nearest Euclidean distance. Each word is then counted and the frequency of each word is stored in a vector $\mathbf{q} \in \mathbb{Z}^n$ where n is the number of visual words. Images in the training set each have a corresponding frequency vector and are used to train the linear SVM classifier.

The training goal of a linear SVM is to find a hyperplane that provides the maximum margin of separation between classes. Let the training set consist of k points $(\mathbf{q}_i, y_i)$ indexed by i where y_i determines if the word frequency vector belongs to the given class. If it belongs to the class then $y_i = 1$ otherwise $y_i = -1$. Any hyperplane that separates the data can be described by all vectors, $\mathbf{h}$, that satisfy $\mathbf{w} \cdot \mathbf{h} - b = 0$ where $\mathbf{w}$ is the vector normal to the hyperplane and b is a scalar bias. The solution for the optimal hyperplane is achieved through quadratic programming using the constraints in Equation 1.4.

$$\begin{aligned} &\min_{\mathbf{w},\mathbf{b},\xi} \left\{ \frac{1}{2}||\mathbf{w}||^2 - p\sum_{i=1}^{k} \xi_i \right\} \\ \text{subject to} \quad & y_i(\mathbf{w}^T\mathbf{q}_i + b) \geq 1 - \xi_i \\ & \xi_i \geq 0 \end{aligned} \tag{1.4}$$

Where $p > 0$ is the penalty parameter of the error term. A more complete and generalized introduction to SVMs is provided in [12]. Once a hyperplane is computed for each class, the intersections are used to describe the decision boundaries for the classifier.

1.3.4 Heterogeneous Classification

In order to classify a heterogeneous terrain image, it is necessary to generate features with an approximately constant density across all pixels. This is achieved by dividing the image into squares and applying feature extraction on each square independently. The feature sets for each square are then combined

Table 1.1: Heterogeneous Classification Definitions

Symbol	**Description**
I	Input image, $I \in \mathbb{R}^{m \times n}$
C	Set of classification centers (pixels) where $C \subset \mathbb{R}^2$
r, r_o	Radius in (fractional) pixels, $r, r_o \in \mathbb{R}$
F	The set of all features for an image I
$F_{\mathbf{c},r}$	All features around $\mathbf{c} \in C$ with radius $\|\|\mathbf{c}\|\| < r$
L	The set of all class labels in the dataset
V_ℓ	Matrix of votes for label $\ell \in L$, $V_\ell \in \mathbb{Z}^{m \times n}$
R	Matrix with classification results, $R \in \mathbb{Z}^{m \times n}$
s_a	Grid spacing for feature extraction in pixels
s_b	Grid spacing for classification points in pixels
$\mathbf{n}$	Desired range (min/max) of features within radius, $\mathbf{n} \in \mathbb{Z}^2$

to form a single feature set. Afterwards, points on the image are selected on a constant grid and classification is performed in each neighboring region. At each point we iteratively resize a ball so that it encompasses the target number of features (within some tolerance). This procedure is very similar to the gradient descent inspired algorithm mentioned in Section 1.3.1. Let r_i represent the radius of the ball at the *ith* iteration and let $D(r_i)$ represent the number of features exclusively inside the ball. The term $D(r')$ is the desired number of features where r' is the unknown radius of interest. To find r' we use Equation 1.5 which includes a user selectable update rate, α.

$$r_{i+1} = r_i + \alpha \frac{D(r_i) - D(r')}{|r_i - r_{i-1}|} \tag{1.5}$$

Once a suitable number of features is encircled, a word histogram vector is generated, and classification is performed using the linear SVM classifier trained on homogeneous terrain images. All pixels exclusively in the circle are labeled with the classification result and this step is repeated about each point. Afterwards a voting procedure is applied to each pixel by tallying the number of votes for each class. This procedure is outlined in pseudo code in Algorithm 1.

Algorithm 1 Heterogeneous Terrain Classification

```
1   $r \leftarrow r_o$
2   $F \leftarrow$ ExtractGridFeatures($I, s_a$)
3   $C \leftarrow$ GenerateClassificationPoints($I, s_b$)
4   for all $\mathbf{c} \in C$ do
5       $(F_{\mathbf{c},r}, r) \leftarrow$ FindRegionalFeatures($C, F, \mathbf{n}, r$)
6       $\ell \leftarrow$ Classify($F_{cr}$)
7       $V_\ell \leftarrow$ Vote($V_\ell, c, r$)
8   end for
9   for all $\ell \in L$ do
10      $R \leftarrow$ CountVotes($V_\ell, R$)
11  end for
```

1.4 Software Architecture

The following section describes the high-level software architecture used in this work. The reader who is more interested in the experiments and results can skip to Section 1.5.

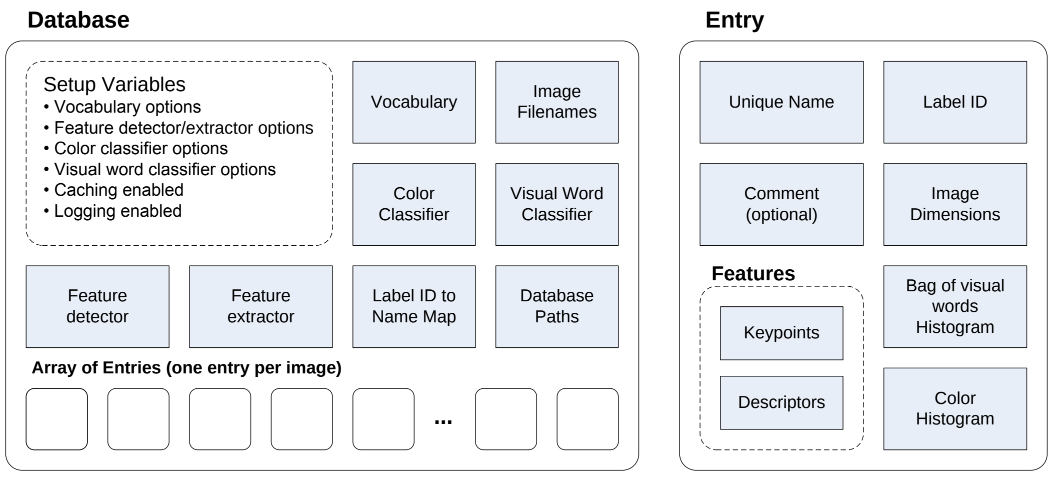

Figure 1.3: Data Oraganization

1.4.1 Structural Organization

The object-oriented software architecture is designed with modularity, expandability, and efficiency in mind. Figure 1.3 shows the high-level organization of the system's data structures. Each **entry**, which is derived from a single image, is organized into a **database** that is initialized using an XML setup file. The database contains all high-level setup variables including vocabulary, feature, and classifier options as well as flags that determine caching and logging behavior. All necessary data structures and functions related to feature extraction, vocabulary generation, and classification are stored in the database. Entries associated with a particular dataset are stored in a dynamic array as part of the database. An entry must be initialized with a unique name and a label ID, and all other entry data can be instantiated afterwards. In this manner only the necessary task-specific data is stored. Consequently, a database that only needs to classify terrain based on color does not need to store feature data in each entry. For space and time efficiency only the identification number corresponding to a verbal label is stored in an entry. The name is translated via an ID to name map in the database. This organization structure is convenient for our supervised learning approach in that a one labeled database can be created as a training set and the other can be created as a test set. The test set can then be easily verified against the training set and verification statistics can be readily computed. In the case where an unlabeled image needs to be classified an independent entry with a null label ID can be classified against a database. If a vocabulary is available then only the visual word histogram needs to be stored in an entry. This makes transmitting and storing entries very memory efficient since the raw descriptors do not need be kept in memory.

1.4.2 Database Initialization

Figure 1.4 represents the initialization procedure for a database which requires the aforementioned XML setup file and database paths. The database paths provide a very convenient way of organizing database images, log output directories, caching directories, and setup files. For example, by changing the caching directory all previous cached data can be preserved while different

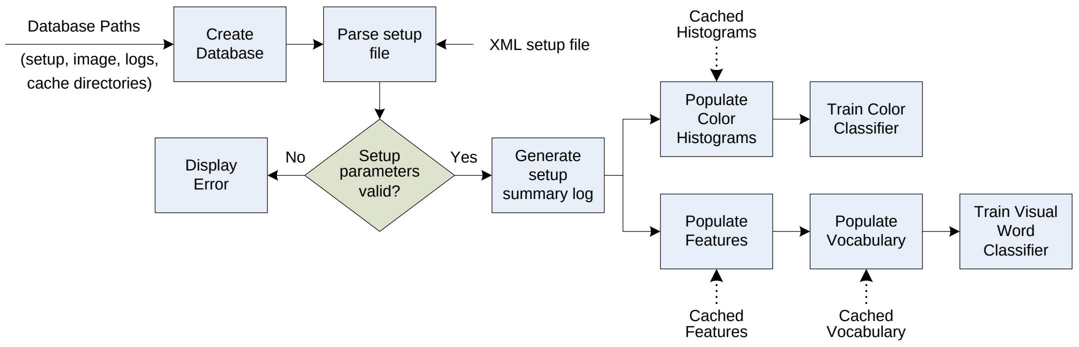

Figure 1.4: Database Initialization Flowchart

settings are used to generate a new database. Most system-level settings can be easily changed in the XML file without having to recompile the software. This provides a very convenient way of running experiments and documenting trials. Once setup parameters have been parsed a time-stamped setup summary is saved to disk containing a list of all parameters used. Afterwards, the color and visual word classifiers are initialized. Setup for the visual word classifier is characterized by three steps: extracting the features, creating a vocabulary, and training the classifier. Preparations for the color classifier consist of populating color histograms and training the classifier. The following sections provide a more detailed explanation of several database initialization tasks.

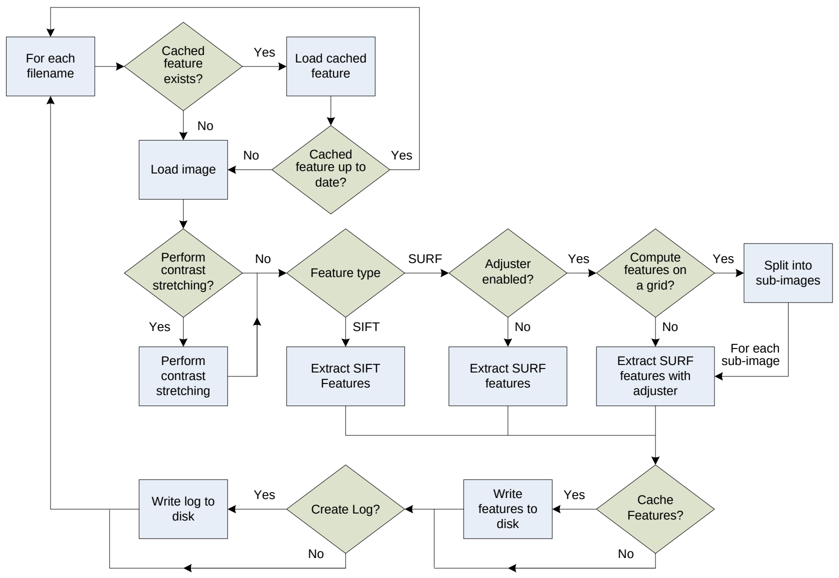

Figure 1.5: Populate Features Flowchart

1.4.3 Populating Features

Feature population (Figure 1.5) starts by iterating through all of the filenames within the database and checking for cached entries. If a cached entry exists and is up to date then the next image filename is processed; otherwise the image is loaded from disk. Once the image is loaded, contrast stretching is performed (if enabled) and feature extraction begins. Our framework supports both SIFT and SURF features, however SIFT features are always computed with a fixed threshold. Under the SURF algorithm features can be extracted using a predetermined Hessian threshold or by using the adjuster algorithm outlined in Section 1.3.1. Optionally the image can be divided into sub-images such that features are extracted from each one. This method is used for the heterogeneous image classification as outlined in Section 1.3.4.

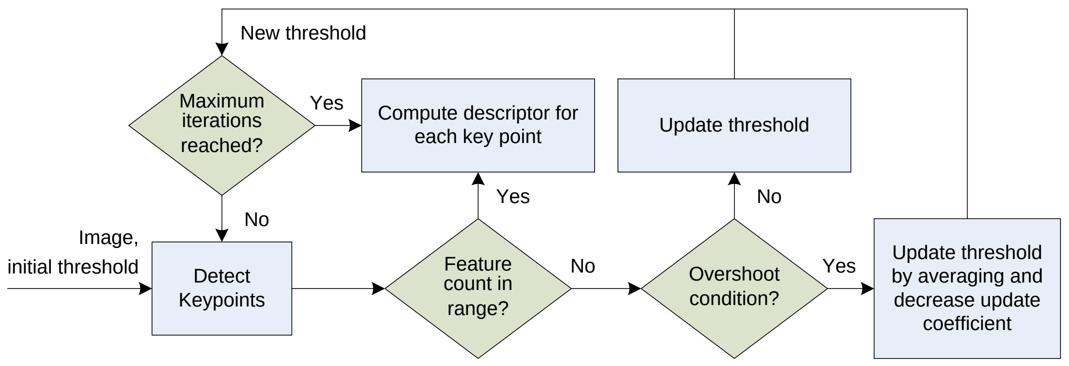

Figure 1.6: Extract Features Flowchart

The threshold adjuster follows the flowchart in Figure 1.6. First, key points are detected (no descriptors are computed) using an initial threshold and their quantity is compared to a desired range. If the quantity is not in the desired range then a check is performed for an overshoot condition. An overshoot condition occurs when the number of key points jumps from too few to too many (or the reverse situation). In such an event the new threshold is set to the average of the current and previous threshold, and the update rate is halved. In the case when no overshoot condition is detected the threshold is updated using the Equation 1.1. The adjuster terminates if the number of iterations exceeds the allowable amount (set by an option in the setup file).

1.4.4 Populating Vocabulary

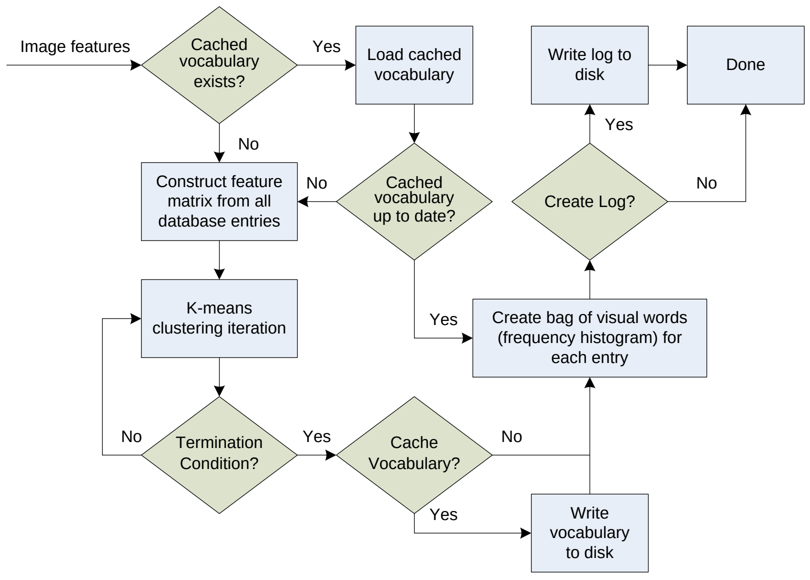
Image features
Cached vocabulary exists?
Yes
Load cached vocabulary
Write log to disk
Done
No
Yes
Construct feature matrix from all database entries
No
Cached vocabulary up to date?
Create Log?
No
K-means clustering iteration
Yes
Create bag of visual words (frequency histogram) for each entry
No
Termination Condition?
Yes
Cache Vocabulary?
No
Yes
Write vocabulary to disk

Figure 1.7: Populate Vocabulary Flowchart

The vocabulary is generated from all features in the particular database and follows the procedure outlined in Figure 1.7. The first step is to check for a valid cached vocabulary and if one exists then k-means clustering is skipped altogether. Otherwise clustering is performed either until cluster groups are no longer reassigned or the maximum number of iterations is reached. The vocabulary is then saved to disk (if the caching flag is enabled), and the bag of visual words is created and stored for each entry as a word frequency histogram. Finally, a log is created to summarize this process and report any pertinent statistics. The software framework presented in this section is modular, efficient, and expandable. It follows a compartmentalized strategy that provides an excellent foundation for testing and future development.

1.5 Offline Experiments

1.5.1 Datasets

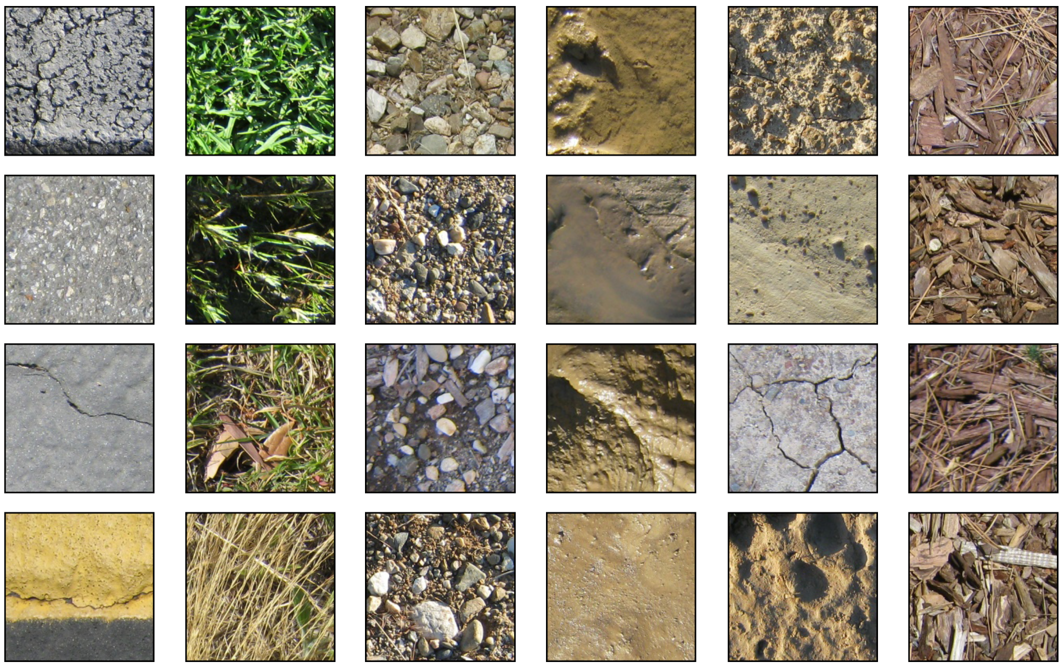
(a) Asphalt (b) Grass (c) Gravel (d) Mud (e) Soil (f) Woodchips

Figure 1.8: Terrain Classes

A large set of outdoor terrain images was used to benchmark our classification algorithms. A 10 megapixel consumer camera was used to take pictures spanning six different terrain types: asphalt, grass, gravel, mud, soil, and woodchips (Figure 1.8). Images were selected to make this dataset challenging to classify with simply color or texture alone. For instance, the asphalt class includes snapshots of pavement and sidewalk with white, yellow, and red painted lines. Many images also contain patches of other terrain. Soil pictures include outcroppings of rocks or weeds, and woodchip images include long pine needles which resemble blades of grass.

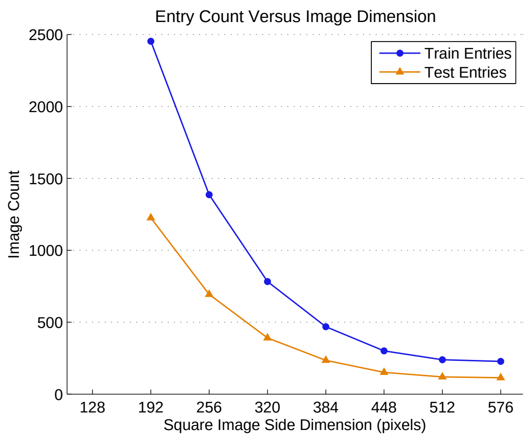

(a) Quantity Versus Size

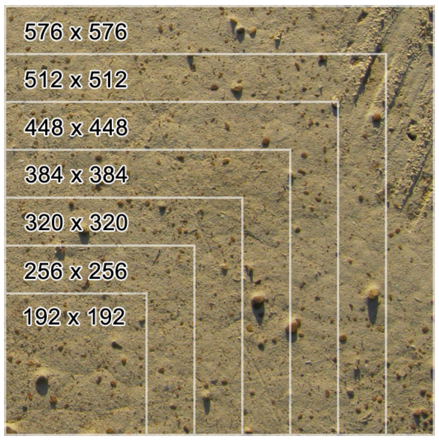

(b) Visual Comparison

Figure 1.9: Dataset Image Dimensions

In total, 63 raw images (summing to 596.85 million pixels) were used to generate the databases. To create a suitably large quantity of entries for testing, each raw camera image was divided into sub-images (Figure 1.8 shows examples from the 192 x 192 pixel dataset). Due to the combined quality degradation of the camera lens, CMOS sensor, and image compression the raw images were down-sampled by halving image dimensions before the subdivision procedure.

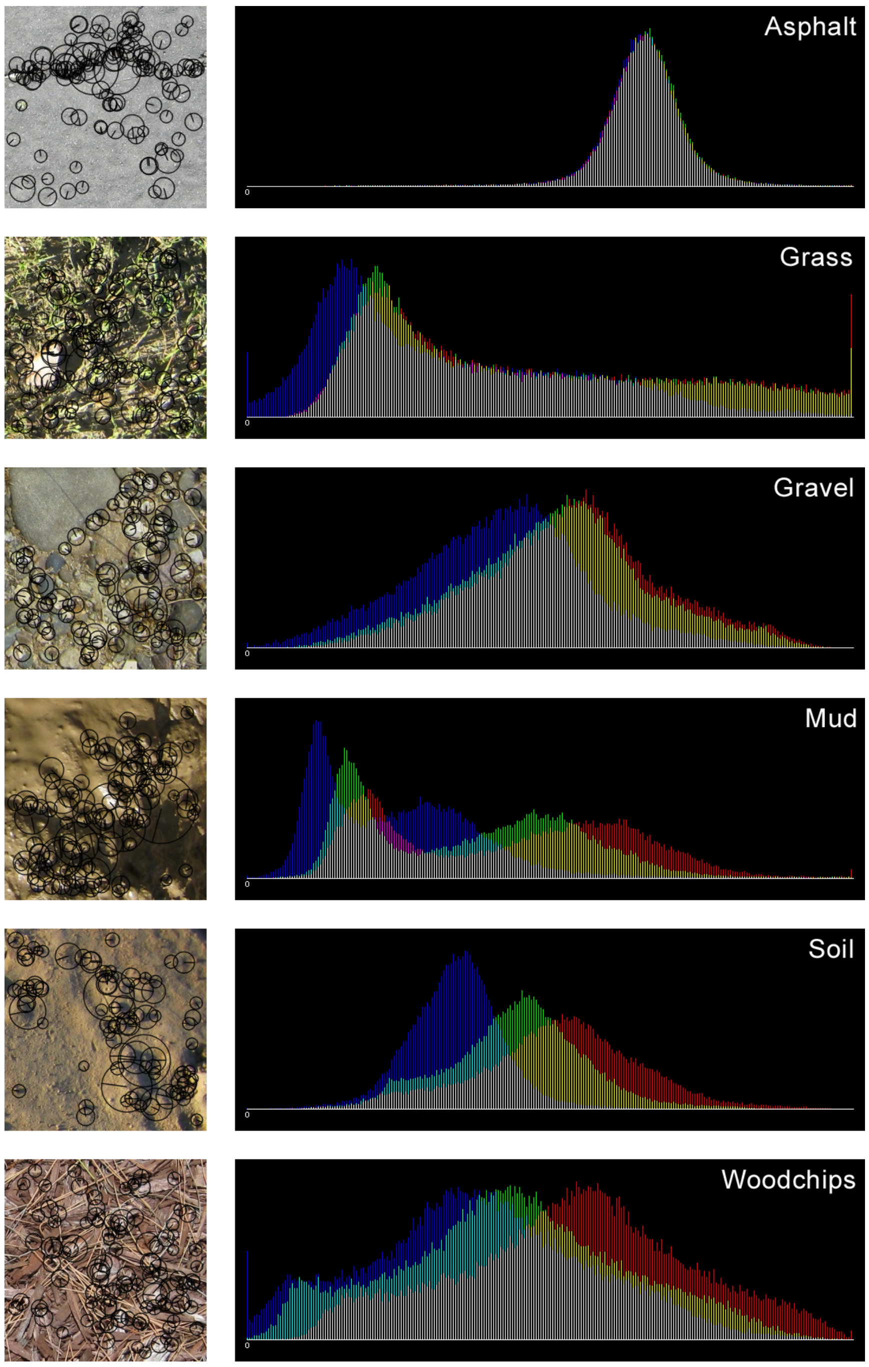

Figure 1.10: Example of SURF key points and color histograms

Seven datasets were created for testing using square images ranging from 192 pixels to 576 pixels in width at 64 pixel increments. In each case, one third of the images were used for training and the rest were used for testing. Figure 1.13(a) shows the number of images in each dataset with respect to image dimension, Figure 1.13(b) shows the relative size of each image dimension, and Figure 1.10 shows the key points and histograms of specific terrain images.

1.5.2 Methodology

The terrain classification framework presents a large number of tunable parameters that impact the performance of feature extraction, vocabulary creation, and classification. This section includes a detailed overview of experiments performed for improving the verification accuracy. Table 1.2 lists experiments that were conducted by varying a single parameter while fixing all others.

Experiment	**Dataset**	**Parameter**	**Range**	**Incr.**
Vocabulary	384 pixel	Number of vocabulary words	10-400	10
K-means	384 pixel	Number of k-mean iterations	5-200	5
Features	320 pixel	Number of nominal features per image	20-300	10
Size	-	Image size (square dimensions)	192-576	64

Table 1.2: List of Parameter Tuning Experiments

In order to provide a fair comparison between image sizes, the nominal feature density was kept at a constant 1 feature per 640 square pixels in the size experiment. Two sets of verification images were used with the image size experiment. The first consists of unaltered test images selected at random and the second contains identical images that are underexposed via post-processing. This was done to test the robustness of each classification method to changes in lighting. In addition to the above experiments, we compared three aforementioned approaches for generating features: fixed threshold, contrast stretching, and an adaptive threshold adjuster.

1.5.3 Results

We expected the number of visual words in the vocabulary to have a direct correlation with the verification accuracy. Very few words, such as 10, would not allow for the classifier to accurately represent each terrain type. An analogy can be drawn to someone who has a poor verbal vocabulary. He would not be able to describe complex objects adequately which could result in a description that is misinterpreted by another person. On the opposite extreme, if the vocabulary contains too many words it may not necessarily help describe a particular class of images. Naturally, there should be a point of diminishing return if vocabulary words increase past a certain quantity. Our results matched this expectation.

Verification accuracy generally improved with word count up to about 150 words as demonstrated by Figure 1.11.

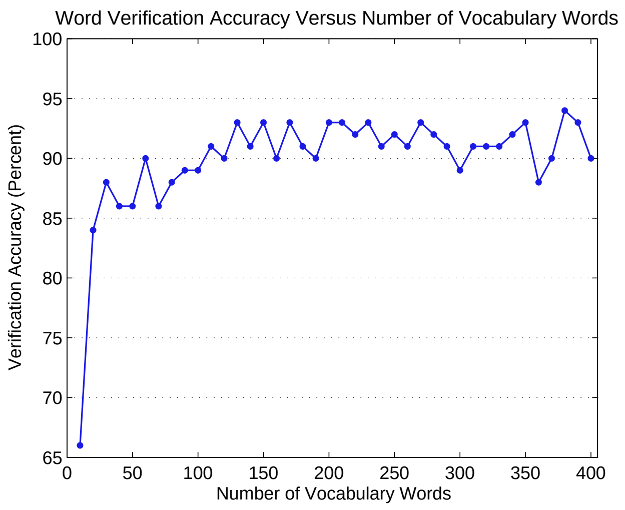

Figure 1.11: Word experiment verification results

We expected the verification accuracy to increase with K-means iterations, but there does not seem to be an obvious method to come up with the necessary number of iterations. Llyod's algorithm will converge in a finite iterations, so we can assume that after a certain point additional iterations will not be beneficial. There has been a lot of work emphasizing the importance of establishing a good visual vocabulary for recognition [19] [18]; however, in this application, the number of clustering iterations had little effect on verification accuracy (Figure 1.12(a)). This is a surprising result and may be due to the broad diversity of descriptors compared to the relatively small number of classes. It may also be that the probabilistic initialization procedure in the k-means++ algorithm is a very effective method for this classification problem. We did not notice a point of diminishing return which suggests the cluster centers did not converge during testing.

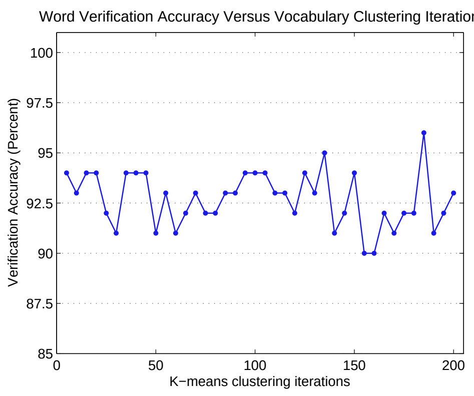

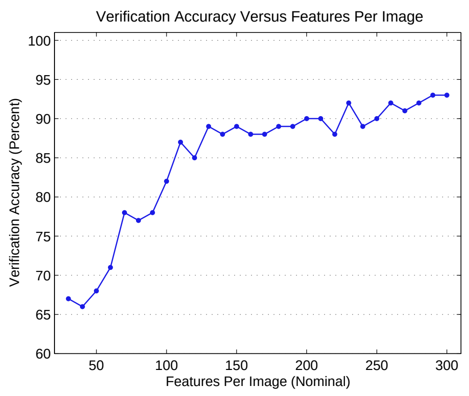

Figure 1.12: K-means (a) and feature experiment (b) results

Similar to the other parameters, we predicted that there needs to be an adequate number of features per image. On the other extreme, too many features per image will introduce noise and redundancy into the system diminishng any further benefits. The results followed our predictions as shown in Figure 1.12(b), and we found that for the 320 pixel dataset between 200-250 features per image produced the best trade-off between size and performance.

Intuition suggests that very small images will not have sufficient data for properly classifying terrain in the image size experiment. This is clear when visually inspecting images smaller than 192x192 pixels because it becomes dif-

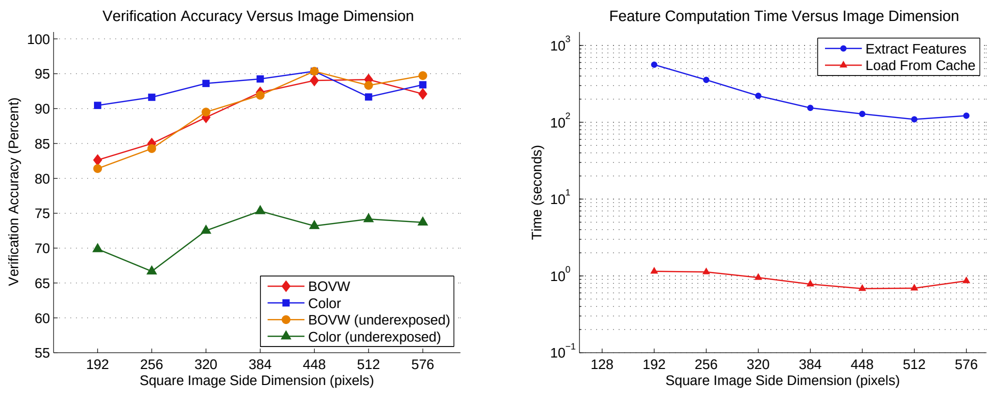

Figure 1.13: Size experiment verification and time performance

ficult, even for a human, to classify them. As image size gets large the classifier will likely train to a very specific set of visual word histograms and we expected to see verification error increase. Results matched our expectations and we observed that the optimal image dimension seems to be 448 x 448 pixels (Figure 1.13). The data also indicates that the color classifier is much less effective in underexposed lighting conditions. This is intuitive because a color histogram simply tallies the color intensity for each pixel and varying illumination alters the color distribution.

The dynamic threshold adjuster proved to be a valuable algorithm because it not only improved verification accuracy, but also greatly decreased memory requirements for the database (Table 1.3). Verification accuracy, compared to a fixed Hessian threshold, improved by 6 percent while the memory requirements decreased by 63 percent. It is important to note that maintaining a nominal number of words per image ensures that the classifier is trained with consistent data and that noise and redundancy is kept to a minimum.

Method	**Verification**	**Size**
Fixed Threshold	89.4%	68.1 Mb
Contrast Stretching	90.7%	53.1 Mb
Dynamic Adjuster	95.4%	25.5 Mb

Table 1.3: Feature Extraction Performance

While there is no straight forward performance metric for heterogeneous terrain classification, our algorithm generated visually intuitive results (Figure 1.14). The algorithm consistently identified homogeneous patches for all classes except for woodchips and gravel. In some cases, boundaries led to misclassification, evident in the bottom row of images. Overall, the algorithm classified images on a fine resolution and generated promising results.

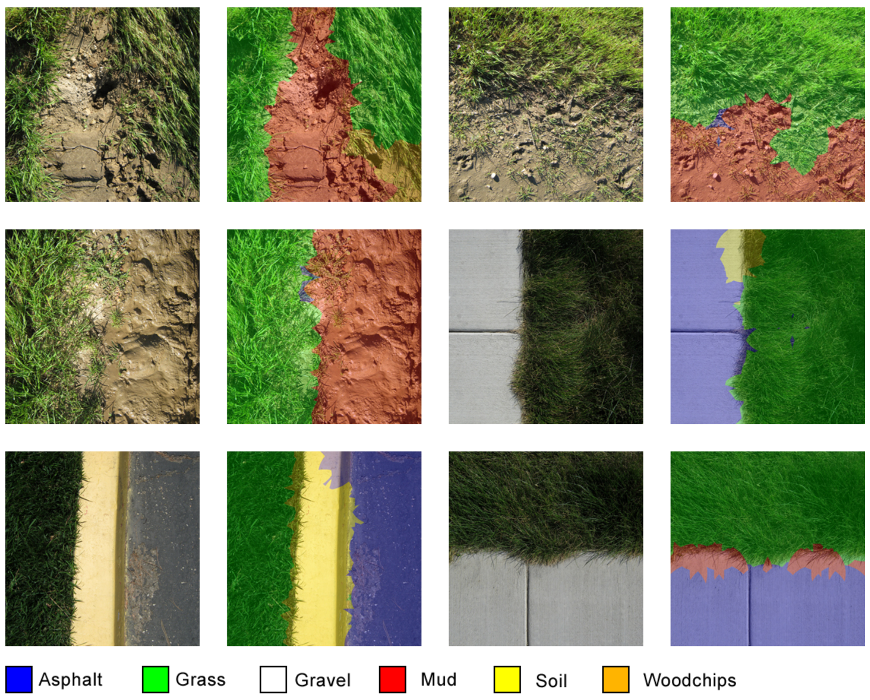

Figure 1.14: Heterogeneous Classification Results

Chapter 2

Applications

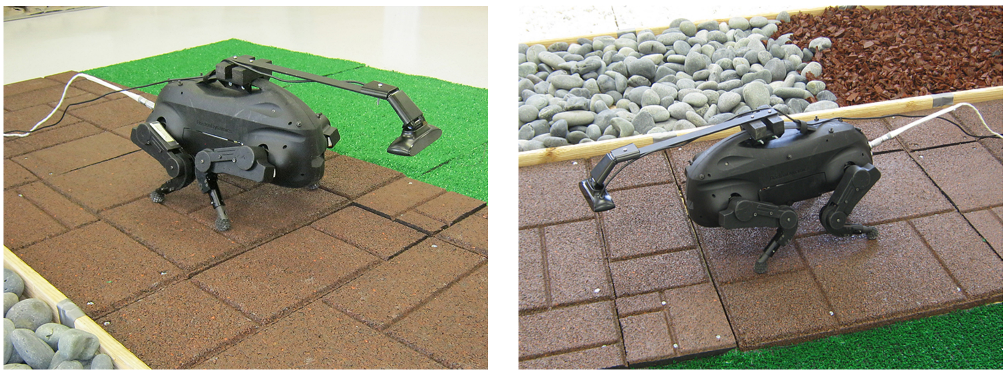

Figure 2.1: Boston Dynamics LittleDog Robot

Boston Dynamics' LittleDog quadruped robot (figure 2.1) was used as the real-time test platform for homogeneous terrain classification. The robot was fitted with a high definition USB webcam with auto-focus capabilities, the Logitech C910. A mid-range laptop was dedicated to terrain classification, and an additional laptop was used to run high-level planning and gait generation. Two machines were used during experimentation to make testing more convenient (dedicated processing, additional screen resolution, etc.), but the framework easily transitions to a single machine.

2.1 System Overview

The software architecture of this system is designed with flexibility and expandability in mind. Each high-level task is encapsulated in its own process, and sockets are used for low-bandwidth intercommunication. This approach allows each task to have dedicated processing power and puts little restriction on the operating system and the development language of each sub-system. Likewise all processes can be run on the same machine and share the same system hardware. Socket communication can also seamlessly transition from a wired hardware layer to a wireless one. The tasks in this system consist of high-level planning, terrain classification, and gait generation.

2.1.1 High-level planning

This system is coordinated by a simple Matlab script that schedules terrain classification and selects the gait regime. The script communicates with the other processes using TC/IP sockets found in the Instrument Control Toolbox.

Classification and gait selection can be broken down into series of cycles as illustrated by figure 2.2.

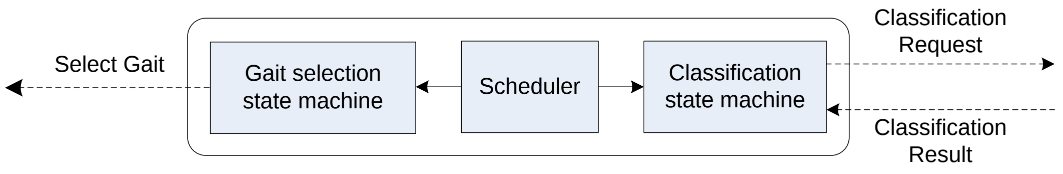

Figure 2.2: Matlab Process

LittleDog starts off each classification cycle in the current gait (in the first cycle this is simply a halted pose) and pauses to initiate terrain classification. The pause is necessary because we encountered image motion blurring problems with our camera due to low shutter speed as well as the rolling shutter effect. Blurring causes some of the most drastic performance degradations to feature based classifiers. In fact the work in [20] addresses this particular problem and presents deblurring methods for computing descriptors. An adequately long pause is required for the camera to stop shaking and the pause is held after initiating classification to ensure system latency does not cause a picture to be taken during movement. After pausing the current gait is continued because the robot has not reached the new terrain. Once it reaches the terrain that has been classified, LittleDog executes the new gait.

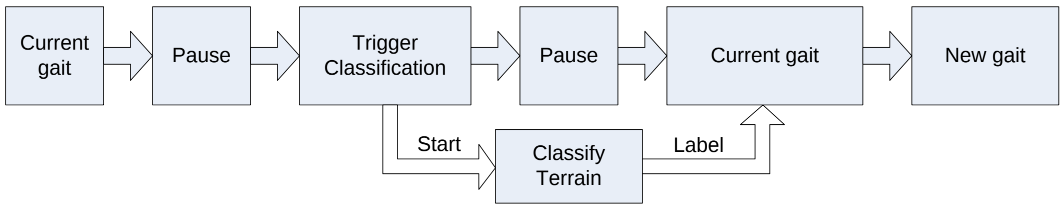

Figure 2.3: Real-time Execution Cycle

2.1.2 Terrain Classification

The terrain classification process (figure 2.4) uses an event-driven framework that includes a graphical user interface (GUI) front-end. The GUI primarily acts as a user monitoring tool for viewing the image input as well as the status of the terrain classification process. Socket communication is handled using an event driven server-client model. The terrain classification process acts as a server which listens on a predetermined port and switches to a unique, dedicated socket once a connection has been established. To simplify networking operations each client request is initiated by opening and subsequently closing the socket connection. The front-end system lets the user load an XML setup file to establish a terrain classification database. Once the setup file is loaded, the terrain classification library is created and the standard initialization sequence is performed as outlined in Section 1.4.2. A fixed interval ”snapshot” timer is then used to sample camera images such that the current image is saved to memory and displayed in the GUI. When a terrain classification event is triggered the latest image is selected for classification and the threshold adjuster algorithm is used to compute features. Each feature is then labeled using visual words from the database dictionary and each word is tallied to generate a histogram. The histogram is then passed to the support vector machine classifier which returns an image label.

Thread support, socket communication and most GUI elements were implemented using the wxWidgets software library. All other image processing and display functionality was implemented using the OpenCV software library. Both libraries are open-source and cross-platform compatible under Linux and Windows.

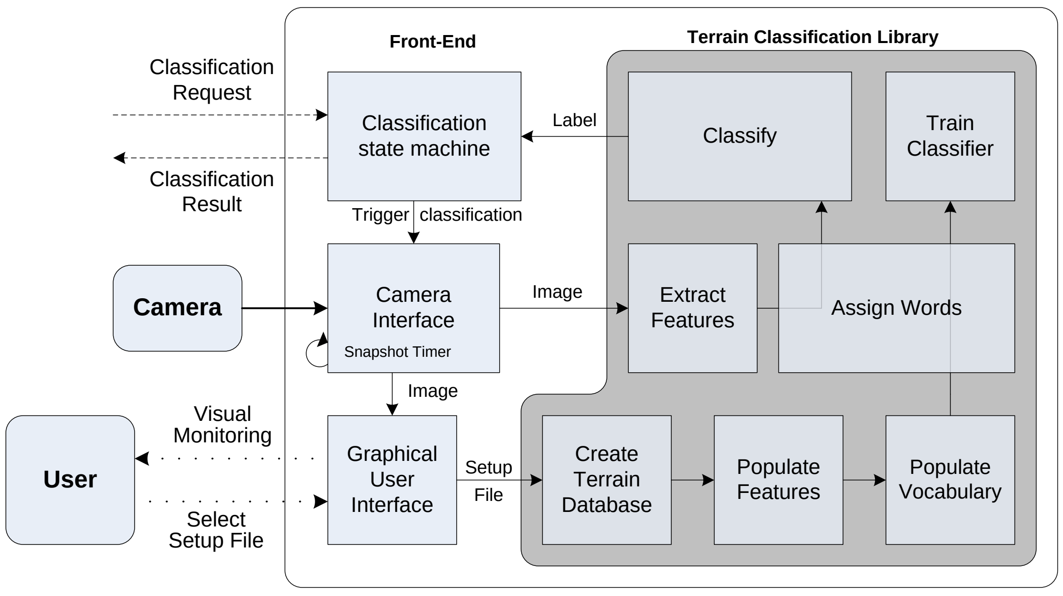

Figure 2.4: Terrain Classification Process

2.1.3 Gait Generation

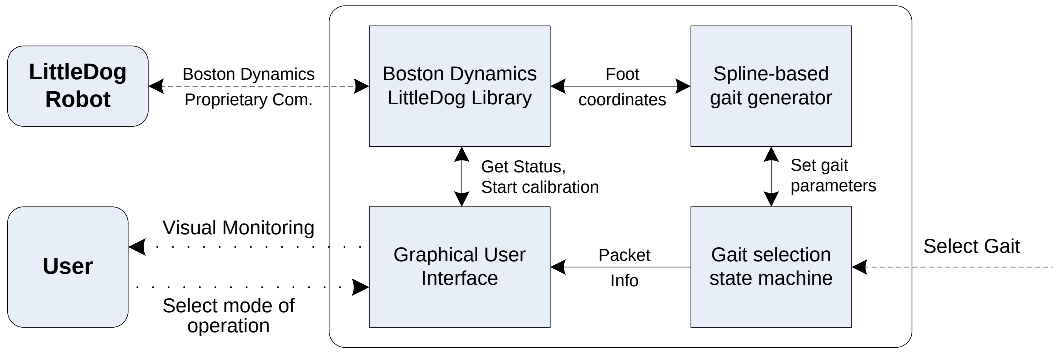
LittleDog Robot
Boston Dynamics Proprietary Com.
Boston Dynamics LittleDog Library
Foot coordinates
Spline-based gait generator
Get Status, Start calibration
Set gait parameters
User
Visual Monitoring
Select mode of operation
Graphical User Interface
Packet Info
Gait selection state machine
Select Gait

Figure 2.5: Gait Generation Process

Gait generation was handled by an independent process (figure 2.5) which selects from several pre-generated gait patterns. A relatively simple set of open-loop gaits was adapted from the Boston Dynamics gait generation example. The following is a high-level overview of the gait pattern used during testing. Each leg on LittleDog is physically identical, so the same fundamental motion is applied to each joint, but mirrored and offset in time. The fundamental motion consists of seven key coordinates in Euclidean three-space: two stance points and five swing points. Each point is also paired with a desired time and then interpolated by a spline. The LittleDog interface library then computes the inverse kinematics for each interpolated coordinate and moves the legs to the desired location. In addition to the fundamental motion, a sinusoidal sway is added to quadruped body to increase stability by adjusting the zero moment point (ZMP). Gait A is reserved for the default Boston Dynamics parameters, however this gait does not demonstrate any advantageous characteristics, and it is only suitable for a nearly flat walking surface. Consequently, it is not used during testing. Gait D is optimized for speed on relatively flat surfaces, gait C is designed for high clearance on rough terrain at the expense of speed, and Gait B is a mixture of the two (figure 2.6).

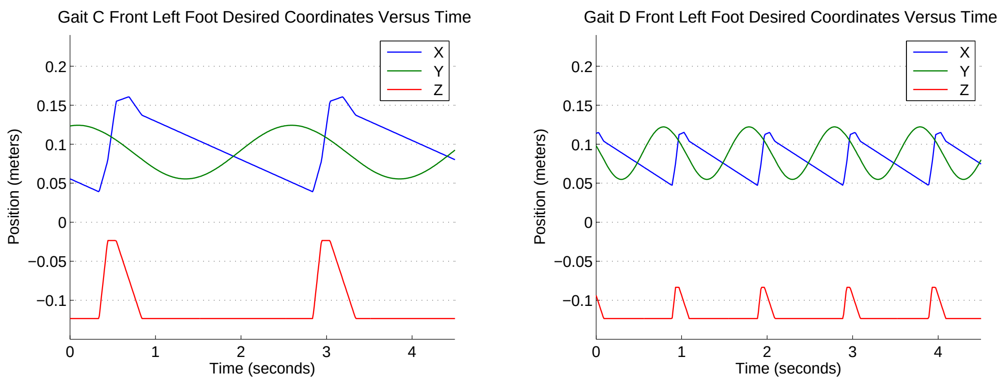

Figure 2.6: LittleDog Gaits

2.2 Real-Time Experiments

2.2.1 Procedures

In order to create a controlled test environment several 2-by-2 foot terrain boards/containers were created to mimic five natural terrain types. Figure 2.7 shows close-up images of each terrain type taken using the Logitech C910 we-

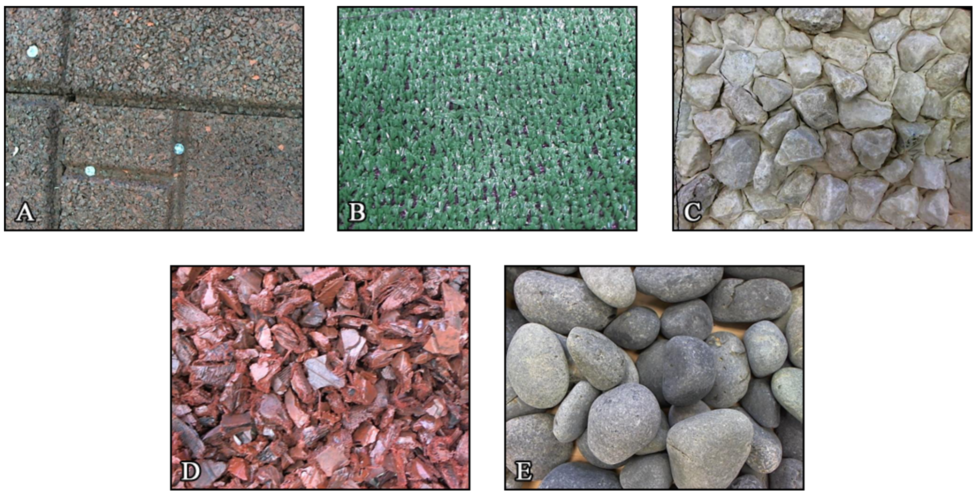

Figure 2.7: LittleDog Experiment Terrain

bcam. The types of terrain were chosen to provide sufficient visual diversity and offer increasingly difficult walking surfaces. The rubber tile terrain (figure 2.7A) vaguely resembles a sidewalk surface and provides the least walking difficultly because it has excellent traction and an even surface. The grass-like surface (B) is also mildly challenging and provides a distinctive texture and color. The small rocks in figure 2.7C are glued to the 2-by-2 boards in order to eliminate slipping, yet they still provide a jagged walking surface. The rubber chips are made from painted recycled car tires resembling a woodchip surface. The woodchip-like terrain is more challenging than the aforementioned terrains because the chips constantly shift around and require high clearance. Lastly, the large rocks, commonly known as Mexican beach pebbles, (Figure 2.7E) present the greatest challenge because are uneven and shift around very easily. Three 2-

by-2 foot terrain boards were each created for the rubber tile, grass, and small rocks. In order to test out a challenging loose terrain transition, the rubber chips and large rocks were put into the same six-by-two foot container.

Initial tests consisted of timing the robot on each type of terrain using each of the three gaits. This established gait performance on every surface and became the basis of gait selection for classification-in-the-loop. After collecting time results the visual terrain classifier was tested on the same four courses. The final course included four terrain types in a 10-by-2 foot area (figure 2.8) and was tested with real time classification. This terrain course was used solely for testing the robustness of the visual classifier. To test visual terrain classification each 2-by-2 foot board was subdivided into a 3-by-3 grid and 640x480 pixel pictures were take of each square. The camera was positioned such that the width of the frame captured the width of each square and it was ensured that no overlapping pixels showed up in any image. Images for both the test and training set were chosen at random with two thirds of the images going to the training set. In addition, a down-sampled set of 320x240 pixel images was created to see how well classification would work with less resolution.

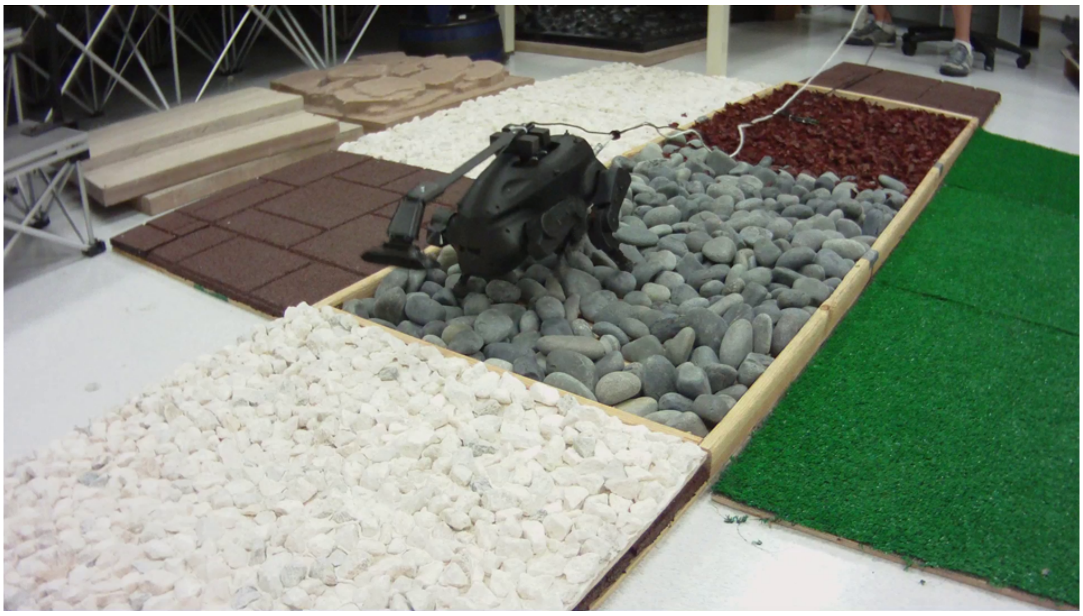

Figure 2.8: LittleDog Traversing the *Large Rocks* Terrain Class

2.2.2 Results

Visually, each terrain is very distinct and offers a great deal of texture so we did not foresee any problems during offline testing. Offline test results confirmed that our experimental terrain was very well suited for classification and we were able get 100% verification accuracy on both the 640x480 image set as well as the 320x240 image set.

		Terrain			
		Small Rocks	**Big Rocks / Rubber Chips**	**Grass**	**Rubber Tile**
Gait	B	22.0	DNC	20.8	20.7
	C	27.7	29.3	26.4	25.8
	D	17.2	DNC	15.8	17.1
	Classify	22.9	44.2	20.4	22.1

Gait D was designed to have very low ground clearance and a relatively fast gait period, so naturally we expected it to perform well on grass and rubber tile. We predicted that LittleDog would not be able to traverse the other terrains because it would stub its feet against the protruding surfaces and veer off course. This was not the case as illustrated by Table 2.2.2, and to the contrary gait D performed the best on all terrain except for big rocks and rubber chips. On the other extreme, our expectation was that Gait C would work reasonably well for every terrain at the expense of speed. This was confirmed by our results, and the only test that took more time was the classification trial for big rocks / rubber chips. We also predicted that Gait B, the hybrid gait, would perform

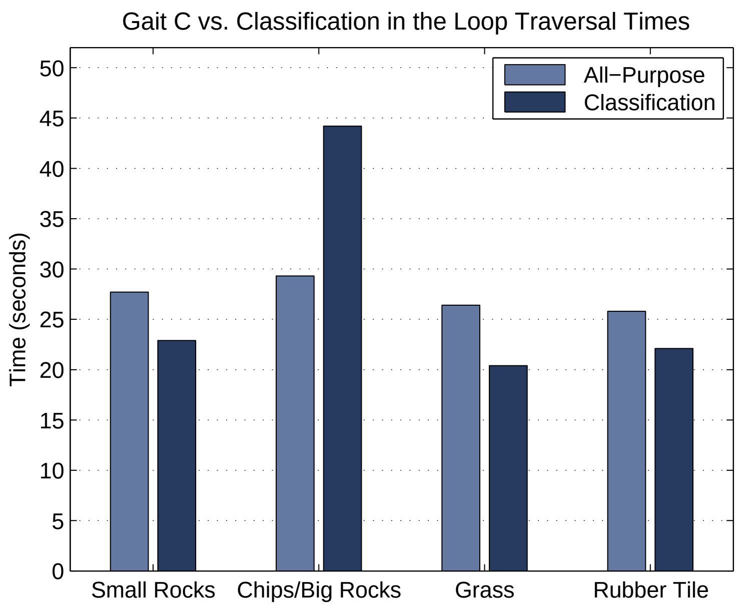

Figure 2.9: Terrain Traversal Performance

the best on the small rock terrain due to its medium clearance and speed. Our results determined that the hybrid gait was actually unnecessary since Gait D performed faster on the small rock terrain.

Figure 2.9 shows a time comparison between Gait C and the classification trial. Results indicate that classification was helpful in all cases except for the most difficult terrain. Classification time was slower in that case due to the stopping requirement. If this requirement did not exist, we would expect to see a nearly identical time as Gait C.

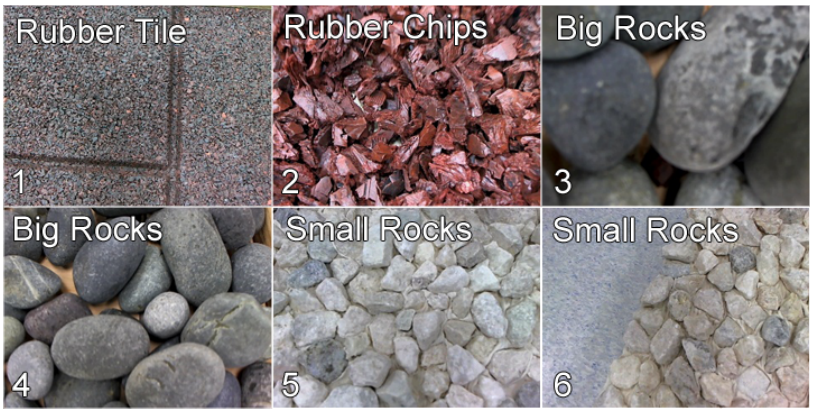

Figure 2.10: Real Time Classification Results

During real time testing the camera auto-focus did not immediately react to changes in object distance. LittleDog would, on occasion, tip the camera downward during a stance and cause the picture to go slightly out of focus. Image blurring decreases the performance of the fast Hessian feature detector so we expected to see some misclassifications. Figure 2.10 shows a consecutive classification trial that was performed on four types of terrain. Tests showed that the classifier was in fact robust enough to minor image blurring (as demonstrated by image 3), and in general there was a very low incidence of misclassifications.

2.3 Conclusion

We developed several novel algorithms that assist popular feature-based recognition techniques. Feature extraction was improved with our gradient descent inspired detection algorithm. Extracting a target number of features increased classification accuracy while decreasing memory requirements. A sliding window classifier was also designed to identify patches in heterogeneous terrain images. This technique showed promising offline results, but struggled slightly with terrain boundaries.

This work demonstrated the effectiveness of our feature-based terrain classification framework in offline and real-time testing. Offline experiments provided valuable data on classification performance in a controlled environment. The findings allowed us to select parameters that gave the most desirable mixture of accuracy and performance. Real-time testing showed that our methods effectively aide autonomous navigation on the LittleDog platform. The robot was able to traverse terrain faster with classification-in-the-loop despite requiring stops to prevent camera blurring. The only case where this slowed the robot was on the most difficult terrain which already required the slowest gait. Overall, we demonstrated that our homogeneous classification approach can be effectively used in real-time to aide quadruped navigation.

2.4 Future Work

This paper provides a solid terrain classification foundation for legged robots, but there is an abundance of ideas to continue research. The primary goal of this work was to create a proof of concept and as a result minimal effort was spent on creating computationally efficient algorithms and code. The dynamic feature adjuster is an example of an algorithm that can be recoded for efficiency. The key point detection in the feature adjuster is computed from scratch at each iteration, and perhaps calculations from the first iteration can be leveraged to prevent further processing. In addition, most of the CPU intensive functions are run in a sequential manner and do not utilize the parallel processing capabilities of modern hardware. Many tasks, such as computing features for database entries can be greatly sped up by dedicating concurrent computation threads. The number of concurrent threads can be determined dynamically by looking at the number of idle cores on the current CPU. In addition, there has been a great deal of recent work on GPU-based computer vision libraries. This work relies on several algorithms that can be processed on a GPU to drastically speed up computation time.

The classification results in this work do not have any measure of confidence. The SVM classifier can be used to produce such a confidence level or perhaps the voting step in the sliding window method may be used to assign a measure of agreement. This would simply involve looking at overlapping regions to determine the amount of consensus among each classification result. On a broader scale it would be interesting to try out different classification methods such as boosting and artificial neural networks with the BOVW framework. A hybrid classifier could also be used to combine color with features. It would also be beneficial to compare our approach to popular terrain classification methods. The work in [2] effectively uses textons to classify terrain in a very similar in scope as this paper. Testing their algorithm using our terrain database would give additional insight about the effectiveness of this work.

Bibliography

[1] Y. Alon, A. Ferencz, and A. Shashua. Off-road path following using region classification and geometric projection constraints. In *Computer Vision and Pattern Recognition*, pages 689–696, 2006.

[2] A. Angelova, L. Matthies, D. Helmick, and P. Perona. Fast terrain classification using variable-length representation for autonomous navigation. In *Computer Vision and Pattern Recognition, 2007. CVPR '07. IEEE Conference on*, pages 1–8, June 2007.

[3] D. Arthur and S. Vassilvitskii. K-means++: the advantages of careful seeding. *Proc. of the 8th Annual ACM-SIAM Symposium on Discrete Algorithms*, pages 1027–1035, 2007.

[4] H. Bay, T. Tuytelaars, and L. V. Gool. Surf: Speeded up robust features. In *Proceedings of the ninth European Conference on Computer Vision*, May 2006.

[5] C. Brooks and K. Iagnemma. Vibration-based terrain classification for planetary exploration rovers. *Robotics, IEEE Transactions on*, 21(6):1185 – 1191, dec. 2005.

[6] Y. Cheng, M. Maimone, and L. Matthies. Visual odometry on the mars exploration rovers - a tool to ensure accurate driving and science imaging. *Robotics Automation Magazine, IEEE*, 13(2):54 –62, june 2006.

[7] A. Chilian and H. Hirschmuller. Stereo camera based navigation of mobile robots on rough terrain. *Intelligent Robots and Systems*, pages 4571–4576, 2009.

[8] J. D. Crisman and C. E. Thorpe. Color vision for road following. In *Vision and Navigation: The CMU Navlab, C. Thorpe (Ed*, pages 9–24. Kluwer Academic Publishers, 1988.

[9] G. Csurka, C. R. Dance, L. Fan, J. Willamowski, and C. Bray. Visual categorization with bags of keypoints. In *Workshop on Statistical Learning in Computer Vision, ECCV*, pages 1–22, 2004.

[10] T. Deselaers, L. Pimenidis, and H. Ney. Bag-of-visual-words models for adult image classification and filtering. In *Pattern Recognition, 2008. ICPR 2008. 19th International Conference on*, pages 1–4, dec. 2008.

[11] S. Gammeter, L. Bossard, T. Quack, and L. V. Gool. I know what you did last summer: object-level auto-annotation of holiday snaps. *International Conf. on Computer Vision*, 2009.

[12] C.-W. Hsu, C.-C. Chang, and C.-J. Lin. A practical guide to support vector classification. `http://www.csie.ntu.edu.tw/~cjlin/papers/guide/guide.pdf`, 2003.

[13] X. Liu and D. Wang. Texture classification using spectral histograms. *IEEE Transactions on Image Processing*, 12:661–669, 2003.

[14] D. G. Lowe. Object recognition from local scale-invariant features. *International Conf. on Computer Vision*, 1999.

[15] M. Luetzeler and S. Baten. Road recognition for a tracked vehicle. *Proc. SPIE Enhanced and Synthetic Vision*, 4023(1):171–180, 2000.

[16] R. Manduchi, A. Castano, A. Talukder, and L. Matthies. Obstacle detection and terrain classification for autonomous off-road navigation. *Autonomous Robots*, 18:81–102, 2004.

[17] C. Manning and H. Schutze. *Foundations of Statistical Natural Language Processing.* MIT Press, May 1999.

[18] D. Nister and H. Stewenius. Scalable recognition with a vocabulary tree. In *IN CVPR*, pages 2161–2168, 2006.

[19] J. Philbin, O. Chum, M. Isard, J. Sivic, and A. Zisserman. Object retrieval with large vocabularies and fast spatial matching. In *Computer Vision and Pattern Recognition, 2007. CVPR '07. IEEE Conference on*, pages 1–8, june 2007.

[20] A. Pretto, E. Menegatti, and E. Pagello. Reliable features matching for humanoid robots. In *Humanoid Robots, 2007 7th IEEE-RAS International Conference on*, pages 532 –538, 29 2007-dec. 1 2007.

[21] N. Sebe, M. S. Lew, and N. Bohrweg. Wavelet based texture classification. In *in International Conference on Pattern Recognition, 2000*, pages 959–962, 2000.

[22] M. Singh and S. Singh. Spatial texture analysis: a comparative study. In *Pattern Recognition, 2002. Proceedings. 16th International Conference on*, volume 1, pages 676 – 679 vol.1, 2002.

[23] S. Thrun, M. Montemerlo, H. Dahlkamp, D. Stavens, and et. al. The robot that won the darpa grand challenge. *Journal of Field Robotics*, 23:661–692, 2006.

[24] J. S. Weszka, C. R. Dyer, and A. Rosenfeld. A comparative study of texture measures for terrain classification. *Systems, Man and Cybernetics, IEEE Transactions on*, SMC-6(4):269 –285, april 1976.